Molecular Orbital Interactions in the Nanostar Dendrimer

Tomofumi Tada, Daijiro Nozaki, Masakazu Kondo, and Kazunari Yoshizawa*

Institute for Materials Chemistry and Engineering, Kyushu University, Fukuoka 812-8581, Japan

Received: August 15, 2003; In Final Form: October 16, 2003

The directional energy flow and intense light emission of the nanostar dendrimer ($C_{460}H_{424}$) that consists of phenylacetylene oligomers and a perylene molecule are studied from the viewpoint of molecular orbital interactions. The method of choice in the present study is the density functional theory and the simple Hückel molecular orbital (MO) method. Although the total density is homogeneous in this π-conjugated system, the amplitude of an individual orbital is localized well in a small fragment, due to the *m*-phenylene joints involved. The highest occupied MO (HOMO) and lowest unoccupied MO (LUMO) are localized well in the perylene core: the HOMO−2, HOMO−1, LUMO+1, and LUMO+2 are localized in the first-generation branches; the HOMO−3 to HOMO−6 and LUMO+3 to LUMO+6 are localized in the second-generation branches; and the HOMO−7 and below and the LUMO+7 and above are localized in the third- and fourth-generation branches. These localized π orbitals play an essential role in the directional, multistep energy flow from the periphery to the center of the nanostar dendrimer. To investigate important photoexcited states of the nanostar dendrimer, singlet excitations of a linear oligomer involved in the dendrimer are calculated with the time-dependent density functional theory. The fragment molecular orbital method is applied to analyze how the orbitals of the nanostar dendrimer are localized in space as well as in energy. A method of reasonable partition of the nanostar dendrimer is theoretically considered in terms of interactions between fragment molecular orbitals.

Introduction

Dendritic molecules[1−6] with highly branched treelike structures have attracted much attention because of their various electrical and optical properties. Photoisomerization with infrared absorption,[7] encapsulation of guest molecules,[8−11] and light-harvesting function[12−14] are interesting properties that derive from the branched nanoscaled structures of dendrimers. Xu and Moore synthesized a well-designed dendrimer ($C_{460}H_{424}$) that consists of phenylacetylene oligomers and a perylene molecule.[12] The dendrimer, which is characterized by the number of generations constructing its unique structure, as indicated in Figure 1, funnels excitation energy from many terminal phenylacetylene fragments to the perylene core and emits fluorescence with high intensity.[15,16] The emission intensity of the dendrimer is 400 times greater than that of isolated 1-ethynylperylene when both molecules are photoexcited by ultraviolet light at 312 nm.[15c] This dendrimer is called "nanostar", which can be viewed as a single-molecular antenna for light and exciton source. Spectroscopic data for similar phenylacetylene dendrimers demonstrated that a generated π-electron−hole pair (exciton) is localized due to the *m*-phenylene joints involved and that the exciton moves smoothly to the core in a directional, multistep manner.[15b,c] These properties result in the directional energy transfer from the periphery to the center of the nanostar dendrimer; absorbed energy in the fourth-generation branches flows into the perylene core via the third-, second-, and first-generation branches in this order. Xu and Moore successfully used an energy level diagram of the nanostar dendrimer to qualitatively understand this directional energy flow.[12]

* Author to whom correspondence should be addressed. E-mail: kazunari@ms.ifoc.kyushu-u.ac.jp.

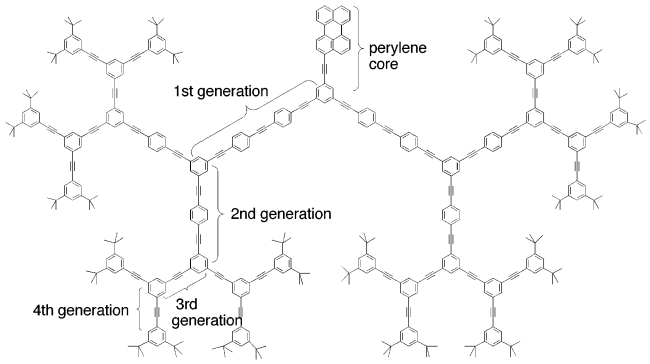

Figure 1. Nanostar dendrimer.

Mukamel and co-workers simulated the absorption spectra and the exciton transport and relaxation processes in the optically excited states of related phenylacetylene dendrimers[17] to analyze important energy-funneling processes in the nanostar dendrimer. How the interesting optical properties derive from the localized electronic excitations is a main issue in these theoretical studies. Nakano, Yamaguchi, and co-workers proposed a mechanism of exciton migration in dendritic molecules to characterize the nonlinear optical properties of phenylacetylene dendrimers.[18] Molecular orbital (MO) calculations have not extensively been used for the characterization of the dendrimer in that it is difficult to anticipate the localized state by inspecting the MOs because the structure is π-conjugated and the orbitals are generally delocalized. However, it is well-known that a *m*-phenylene coupler localizes the molecular orbitals in space while a *p*-phenylene coupler delocalizes the molecular orbitals.[19] Shimoi and Friedman carried out MO calculations to look at the origin of the localized state in meta-linked phenylene dendrimers.[20] Although their models do not involve acetylene blocks that are

10.1021/jp0309724 CCC: $25.00
Published on Web 12/02/2003

essential for the nanostar dendrimer to stabilize its planar structure, they reasonably obtained relevant localized levels using MO calculations and concluded that the electron−hole interaction is not necessary for the localized electronic excitations.

In the present work we reconsidered from simple Hückel MO[21] and density functional theory (DFT)[22,23] calculations the important relationship between the light-harvesting function and the role of the *m*-phenylene joints in the nanostar dendrimer. We used a linear oligomer showing a directional and multistep energy flow and calculated the excitation energies and oscillator strengths of the oligomer with the time-dependent DFT (TDDFT)[24−26] to gain a useful insight into excited states of the nanostar dendrimer. In the analysis of the energy migration in the nanostar dendrimer we employed the Hückel MO method. Although light-induced excitations generate electron−hole pairs, we can reasonably restrict our discussion to the migration of electron in unoccupied levels because of the electron−hole symmetry in the π-electron approximation we adopted. We used the fragment molecular orbital (FMO) method[27] to highlight how the MOs of the nanostar dendrimer are localized by the *m*-phenylene joints.

Molecular Orbital Diagrams and Analysis of Singlet Excited States

To determine the structure of the nanostar dendrimer indicated in Figure 1, we first performed a full geometry optimization with the PM3 method,[28] which is the most reliable semiempirical MO method for the determination of organic molecular geometries, using Gaussian 98,[29] and found this molecule to be nearly planar. Thus, the acetylene couplers play an essential role in relaxing the repulsion between neighboring benzene rings, especially the ortho H−H interactions. The optimized Cartesian coordinates can be seen in Table 1S of the Supporting Information. Thus, we can reasonably assume the nanostar dendrimer to be planar in our theoretical considerations. We performed simple Hückel MO calculations to look in detail at the MOs and orbital interactions. Figure 2 shows frontier π MOs of the nanostar dendrimer. Although the total density is homogeneous in space in this kind of π-conjugated hydrocarbons, the amplitude of an individual orbital is not homogeneous in general.[30] The highest occupied MO (HOMO) and the lowest unoccupied MO (LUMO) are localized well in the perylene core: the HOMO−2, HOMO−1, LUMO+1, and LUMO+2 are localized in the first-generation branches; the HOMO−3 to HOMO−6 and LUMO+3 to LUMO+6 are localized in the second-generation branches; and the HOMO−18 to HOMO−7 and the LUMO+7 to LUMO+18 are localized in the third- and fourth-generation branches. Clearly, these nicely localized π MOs, which derive from the symmetry restriction caused by the *m*-phenylene joints,[19,20] should have significant relevance to the directional, multistep energy flow in the nanostar dendrimer.

Let us look at a certain case where the LUMO+7, which is localized in the peripheral third- and fourth-generation branches of the nanostar dendrimer, is filled with an electron in a photoexcited state. The electron then descends stepwise in energy and at the same time moves from the peripheral branches to the center. When the electron goes down to the LUMO, which is localized at the perylene core as well as on the neighboring phenylacetylene, through repeated radiationless transitions in a multistep manner, the nanostar dendrimer finally emits fluorescence as a result of the electron−hole recombination at the perylene core. Since as shown in Figure 2 many MOs are

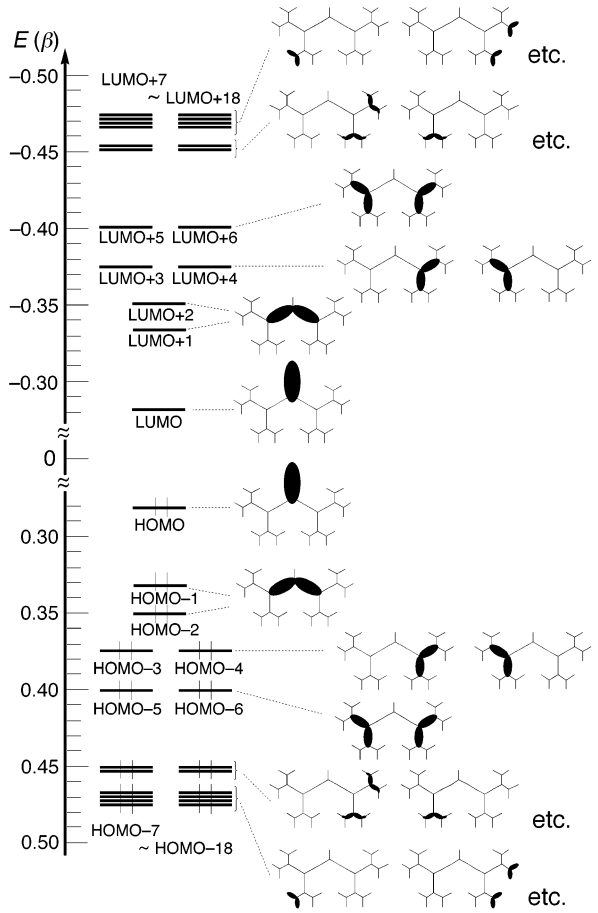

Figure 2. Densities of frontier π MOs for the nanostar dendrimer from a Hückel calculation. The β means the unit of resonance integral, which is generally negative.

localized in the third- and fourth-generation branches as well as in the energy regions of $+0.45\beta$ to $+0.48\beta$ and -0.45β to -0.48β, in which the β is the resonance or the transfer integral in the Hückel method, many electrons excited in the third- and fourth-generation branches migrate to the perylene core. Consequently, intense light emission is observed in the nanostar dendrimer.

To better understand the MO diagram of the nanostar dendrimer, we used a linear oligomer (molecule **1** shown in Figure 3) that consists of the perylene core, the first-, second-, third-, and fourth-generation branches. Figure 3 also shows several fragments involved in molecule **1**, in which the names of the fragments are followed by Mukamel's nomenclature.[17a] P1, P2, and P3 involve two, three, and four benzene rings, respectively, linked linearly in the para positions with acetylene couplers; M2 and M3 involve three and four benzene rings, respectively, linked bent due to the *m*-phenylene joint; and PP involves a perylene molecule and a benzene ring, linked with an acetylene coupler.

As shown in Figure 4, the MOs of **1** are localized in space as in the nanostar dendrimer, due to the *m*-phenylene joints. Let us look at the unoccupied levels because a photoexcited electron is housed in an unoccupied level while a hole is housed in an occupied level. As we go down from the LUMO+4 to the LUMO, the localized orbital amplitude moves from the M2 to PP fragments. Therefore an excited electron housed in an unoccupied MO after photoexcitation should move from the terminal phenylacetylene fragment to the perylene core as in the nanostar dendrimer. Further analyses of molecule **1** are helpful for a better understanding of the directional energy

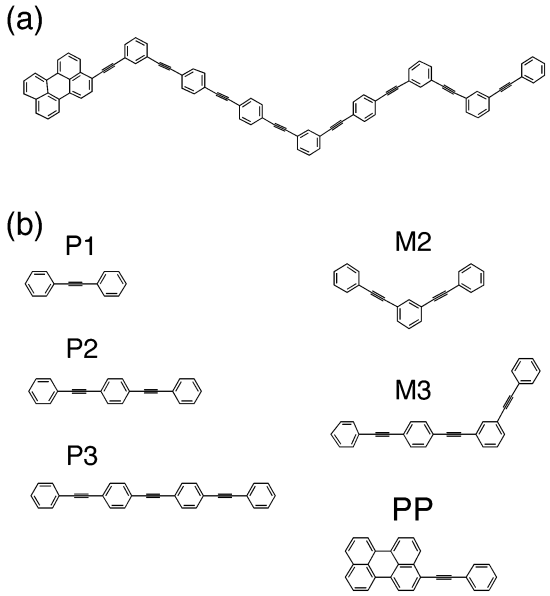

Figure 3. (a) Molecule **1** and (b) its fragments obtained by partitioning in the *m*-phenylene joints. P means a fragment including *p*-phenylene joints, and M a fragment including a *m*-phenylene joint. PP is the perylene core.

transfer in the nanostar dendrimer. To consider photoexcited states of molecule **1** in detail, we performed a TDDFT calculation at the B3LYP[31] level with the 6-31G(d,p)[32,33] basis set and obtained 30 singlet excitations. Table 2S of the Supporting Information lists computed excitation energies, oscillator strengths, and configurational composition. Eighteen π-MOs (the HOMO−9, HOMO−8, HOMO−6 to LUMO+6, LUMO+8, and LUMO+16) mainly take part in the singlet excitations; Figure 1S of the Supporting Information shows these π-MOs schematically. These frontier orbitals are localized well and the orbital phases are similar to those from the Hückel method. Figure 5 shows a schematic representation of computed singlet excitations by the light at 315, 314, and 313 nm. The excitation by the light at 314 nm mainly takes place in the terminal region of molecule **1** (i.e., the excitation from the HOMO−3 to the LUMO+5) and has no direct correlation with the perylene core. We confirmed from detailed analysis that this type of excitation occurs only upon irradiation at 314 nm. Shortreed and co-workers reported that the photoexcitation by the light at 312 nm results in the directional energy transfer in the nanostar dendrimer and that the perylene core in the nanostar dendrimer does not correlate with the photoexcitation.[15c] Therefore we can reasonably say that the excitation by the light at 314 nm computed with B3LYP/6-31G(d,p) corresponds to the observed photoexcitation at 312 nm that leads to the directional energy flow in the nanostar. The computed excited state is composed not only of the terminal-to-terminal excitation but also of the first- to second- and the terminal- to second-generation excitations as shown in Figure 5b, and thus electrons excited at the second generation as well as at the terminal fragments will mainly contribute to the directional, multistep energy flow in molecule **1**.

To derive significant features in the localized orbitals, let us again consider the MO diagram for molecule **1**. How do the MOs of **1** correlate with the MOs of the small fragments? Figure 4b shows the HOMOs and LUMOs of the phenylacetylene fragments that construct molecule **1**. The orbital energies and phases of the LUMO, LUMO+1, and LUMO+2 of molecule **1** are in good agreement with those of the LUMOs of the PP, P3, and P2 fragments, which clearly shows that these fragments have no orbital interactions with neighboring moieties in molecule **1**. Although we expect that the LUMO+3 of molecule **1** should correlate with the LUMO of P1, it apparently derives from the M2 fragment. This result tells us that the P1 fragment is not independent in molecule **1**.

Let us consider the M3 and M2 fragments shown in Figure 3b to find a good way of partitioning phenylacetylene oligomers into small fragments. In Figure 6 we show the HOMO−1, HOMO, LUMO, and LUMO+1 of M3. Both Hückel and B3LYP/6-31G(d,p) calculations give essentially identical orbitals and show that the MOs of M3 are localized in the fragments connected in the *p*-phenylene joints. The HOMO and LUMO of M3 strongly correlate with the HOMO and LUMO of P2 in energy as well as orbital phase, and the HOMO−1 and LUMO+1 of M3 correlate with the HOMO and LUMO of P1; see Figure 4b for the HOMOs and LUMOs of P2 and P1. Thus, fragment M3 is still separable in the *m*-phenylene joint into smaller fragments.

Fragment M2 involves three benzene rings linked by acetylene couplers, the three benzene rings being connected by a *m*-phenylene joint at the center. Although M3 and M2 are similar in shape, their frontier orbitals are very different. Figure 7 shows the HOMO−1, HOMO, LUMO, and LUMO+1 of M2 from Hückel and B3LYP/6-31G(d,p) calculations. The Hückel and DFT orbitals are very similar again. In contrast to M3, these orbitals are fully delocalized on the molecule. This is a direct consequence from the molecular symmetry of M2. Since M2 has a 2-fold axis of symmetry, its MOs are inevitably symmetric or antisymmetric with respect to the 180° rotation around the C_2 axis. In contrast, M3 is at most a C_s molecule that has only a mirror plane, and the MOs of M3 do not undergo such a symmetry restriction. This means that M2 is not separable into independent, smaller fragments any more. To better understand the orbital localization in the nanostar dendrimer, let us apply the FMO method to the M3 and M2 fragments.

Fragment Molecular Orbital Analysis

The FMO method, which was first developed by Fujimoto and Hoffmann,[27] is of great use in understanding orbital interactions in molecules. In this analysis, a molecule is divided into small fragments, and characteristics of molecular orbitals are represented in terms of orbital interactions between fragments.

M3 involves four benzene rings linked by acetylene couplers, the benzene rings being connected by a *m*-phenylene joint. We partitioned M3 in two ways: one is a fragmentation into P2 and phenylacetylene, and the other is a fragmentation into P1 and di(phenylacetylene). Figure 8 shows orbital interaction diagrams for the two kinds of fragmentation for M3 in the framework of the Hückel MO method. Here a significant MO correlation is indicated with a solid line, and a weak correlation is indicated with a broken line. Figure 8a demonstrates that the HOMO and LUMO of P2 have no interactions with any orbitals of phenylacetylene; as a consequence, the HOMO and LUMO of P2 are kept unchanged as the HOMO and LUMO of M3. Since the HOMO and LUMO of P2 have no orbital amplitude in the meta-positions of the terminal benzene rings where a bond is formed with the terminal acetylene carbon of phenylacetylene, they have no orbitals to interact in phenylacetylene. Thus, the energies of the HOMO and LUMO of P2 remain unchanged in the united molecule. This method of partitioning is simpler than the other in that it gives noninteracting fragments. The MOs of P1 and di(phenylacetylene) are mixed well to form the MOs of M3. Figure 8b shows that the HOMO of P1 and di(phenylacetylene) are weakly coupled out-of-phase to result in the

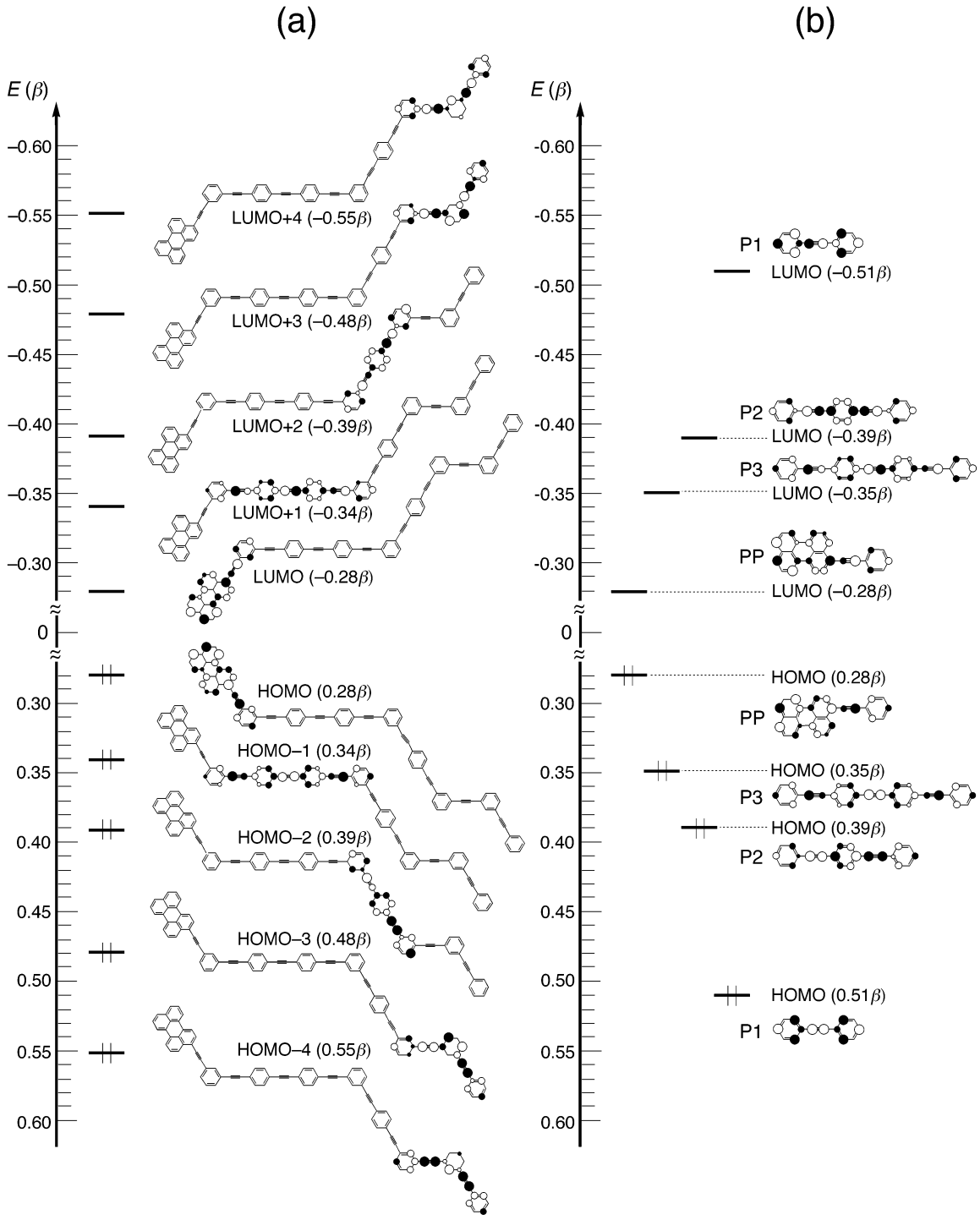

Figure 4. Molecular orbital diagrams for (a) molecule **1** and (b) its fragments partitioned in the *m*-phenylene joints.

HOMO of M3 and that the LUMOs of the two fragments are coupled in-phase to result in the LUMO of M3. Since the HOMO and LUMO of P1 have no orbital amplitude in the meta positions, the HOMO and LUMO of P1 are kept unchanged as the HOMO−1 and LUMO+1 of M3. In any partition the π frontier orbitals of M3 have a significant localized nature inherent in the fragments.

Figure 9 shows an orbital interaction diagram for M2, which is partitioned into phenylacetylene and P1. The MOs of M2 are delocalized. We see from this illustration that the HOMO of M2 derives from an out-of-phase combination of the HOMOs of phenylacetylene and P1 and that the LUMO of M2 derives from an in-phase combination of the LUMOs of phenylacetylene and P1. Thus, the frontier orbitals of the two fragments are highly mixed to form the delocalized orbitals of M2. Consequently, the M2 fragment is not separable any more from the viewpoint of orbital interaction. Since M4 and M6 also have a C_2 axis, their MOs must be symmetric or antisymmetric with respect to the C_2 axis. The MOs of M4 and M6 are also not separable.

We conclude from the results obtained in the FMO analysis of M2 and M3 that the MOs of phenylacetylene oligomers cannot be partitioned with respect to the *m*-phenylene joint when the phenylacetylene oligomers have a C_2 axis in the *m*-phenylene joint. In other words, phenylacetylene oligomers are not separable when they consist of odd-numbered benzene rings

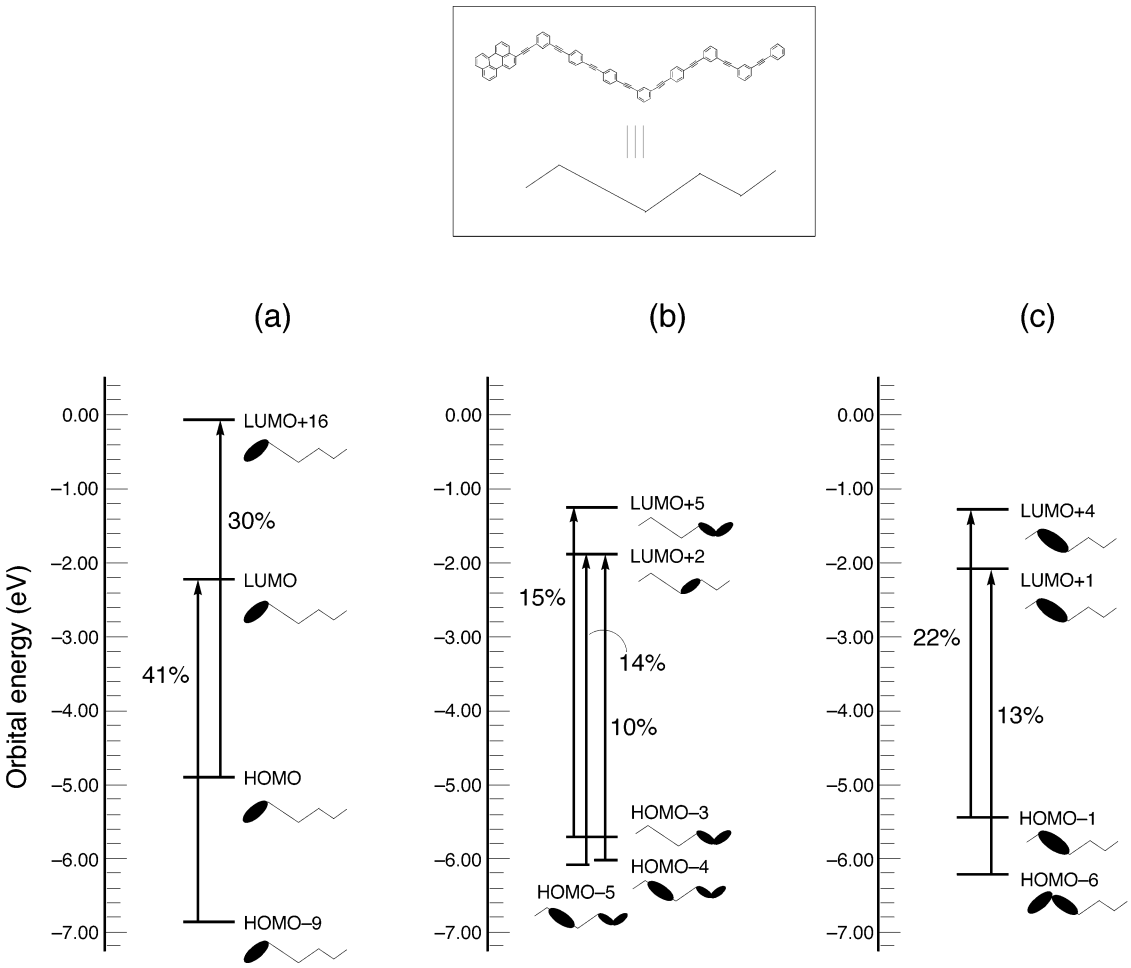

Figure 5. Schematic representation of singlet excitations by the light at (a) 315 (3.94 eV), (b) 314 (3.95 eV), and (c) 313 nm (3.97 eV) obtained from a TDDFT calculation at the B3LYP/6-31G(d,p) level of theory. Configurations contributing more than 10% are shown.

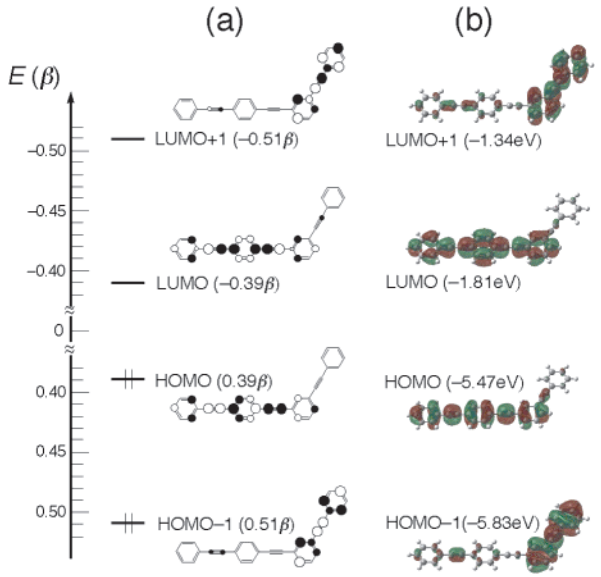

Figure 6. The HOMO−1, HOMO, LUMO, and LUMO+1 of M3 obtained from (a) Hückel and (b) B3LYP/6-31G(d,p) calculations.

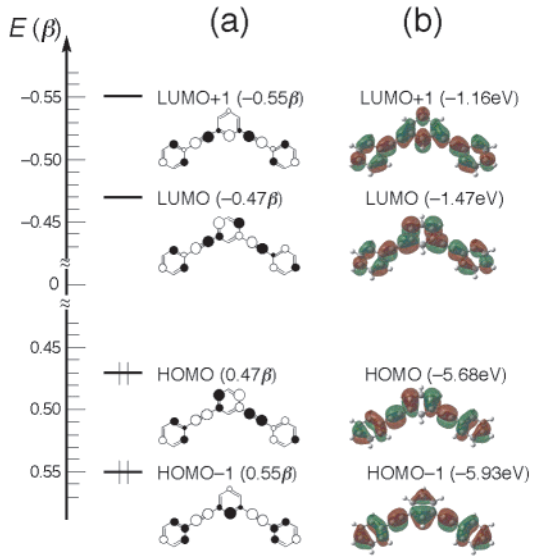

Figure 7. The HOMO−1, HOMO, LUMO, and LUMO+1 of M2 obtained from (a) Hückel and (b) B3LYP/6-31G(d,p) calculations.

that are connected by a *m*-phenylene joint at the center. Accordingly, we can partition molecule **1** into four fragments PP, P3, P2, and M2, as shown in Figure 10. In fact, the MOs of **1** indicated in Figure 4a are localized well on these fragments.

In understanding the interesting optical properties of the nanostar dendrimer, the rule for partitioning phenylacetylene oligomers is applicable. We can partition this molecule into PP, M6, M4 × 2, and M2 × 12, in which the MOs of the nanostar dendrimer are well localized (see Figure 2 again). M6 and M4 are the first- and second-generation branches, respectively, and M2 corresponds to the third- and fourth-generation branches. Table 1 summarizes the degeneracies of the nanostar dendrimer

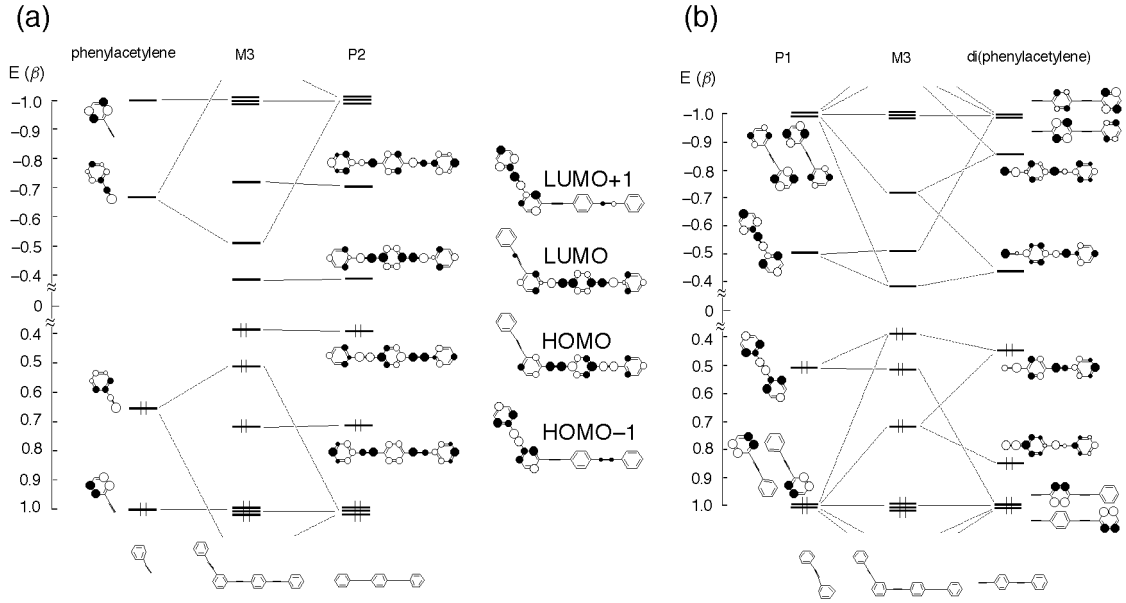

Figure 8. Orbital interaction diagrams for M3 partitioned into (a) phenylacetylene and P2 and (b) P1 and di(phenylacetylene).

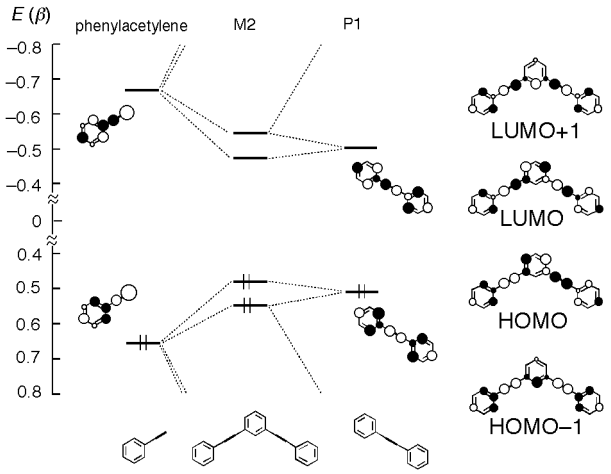

Figure 9. An orbital interaction diagram for M2 partitioned into phenylacetylene and P1.

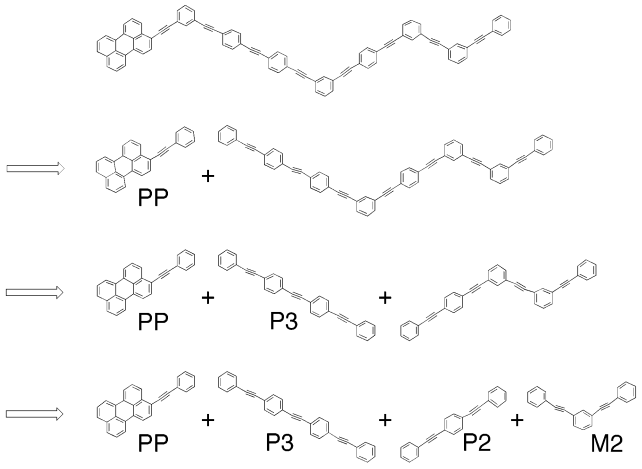

Figure 10. A reasonable partition of molecule **1** into PP, P3, P2, and M2 in the *m*-phenylene joints.

and correlation of the MOs between the nanostar dendrimer and these small fragments in the unoccupied levels. In the energy range of 0 to -0.41β, the orbital energies of the nanostar dendrimer are in good agreement with those of PP, M6, and M4, while the MOs generated from the LUMO of M2 in the nanostar dendrimer split into two groups (i.e., MOs at -0.45β and at -0.47β in energy). The degeneracies of the nanostar dendrimer shown in Table 1 demonstrate that a large number of electrons excited in the second-, third-, and fourth-generation branches migrate to the perylene core in a directional, stepwise manner, and therefore one can obtain light emission with high intensity.

TABLE 1: MO Energies and Degeneracies of the MOs in the Nanostar Dendrimer and Its Fragments

nanostar			fragment	
E (β)	MOs[a]	degeneracy	E (β)	MOs
−0.47	LUMO+11 to LLUMO+18 (4th)	8	−0.47	LUMO (M2)
−0.45	LUMO+7 to LLUMO+10 (3rd)	4	−0.47	LUMO (M2)
−0.41	LUMO+5, LLUMO+6 (2nd)	2	−0.41	LUMO+1 (M4)
−0.37	LUMO+3, LLUMO+4 (2nd)	2	−0.38	LUMO (M4)
−0.35	LUMO+2 (1st)	1	−0.35	LUMO+1 (M6)
−0.33	LUMO+1 (1st)	1	−0.34	LUMO (M6)
−0.28	LUMO (PP)	1	−0.28	LUMO (PP)

[a] Generations in which the orbital amplitude is localized are shown in parentheses.

Conclusions

We have qualitatively considered the energy flow and intense light emission of the nanostar dendrimer from the viewpoint of molecular orbital interactions. Although the total density is generally homogeneous in space in this kind of π-conjugated hydrocarbons, individual orbital density is not homogeneous. The amplitude of each orbital of the nanostar dendrimer is localized well in a small fragment, due to the *m*-phenylene joints. The HOMO and LUMO are localized in the perylene core; the HOMO−2, HOMO−1, LUMO+1, and LUMO+2 are localized in the first-generation branches; the HOMO−3 to HOMO−6 and LUMO+3 to LUMO+6 are localized in the second-generation branches; and the HOMO−7 and below and the LUMO+7 and above are localized in the third- and fourth-generation branches. We calculated the excitation energies of a

linear phenylacetylene oligomer involving the perylene core, the first-, second-, third-, and fourth-generation branches by using TDDFT at the B3LYP/6-31G(d,p) level of theory, and found that electrons excited at the second-, third-, and fourth-generation branches mainly contribute to the directional, multistep energy flow in the nanostar dendrimer. We applied the fragment molecular orbital method to see how the orbitals of the nanostar dendrimer are localized in space as well as in energy. This traditional method in molecular orbital theory helps our understanding of the light-harvesting function of the nanostar dendrimer and shows us a method of reasonable partition of the nanostar dendrimer.

Acknowledgment. K.Y. acknowledges Grants-in-aid for Scientific Research from the Ministry of Education, Culture, Sports, Science and Technology of Japan (MEXT), Japan Society for the Promotion of Science, Japan Science and Technology Cooperation, the Murata Science Foundation, Kyushu University P&P "Green Chemistry", and "Nanotechnology Support Project" of MEXT for their support of this work. Computations were in part carried out at the Computer Center of the Institute for Molecular Science. M.K. thanks JSPS for a graduate fellowship.

Supporting Information Available: Figure 1S of π frontier orbitals of molecule **1** calculated with B3LYP/6-31G(d,p), Table 1S of PM3-optimized Cartesian coordinates for the nanostar dendrimer, and Table 2S of singlet excitation energies, oscillator strength, and configurational composition of molecule **1** calculated with B3LYP/6-31G(d,p). This material is available free of charge via the Internet at http://pubs.acs.org.

References and Notes

(1) (a) Buhleier, E.; Wehner, W.; Vögtle, F. *Synthesis* **1978**, 155. (b) Newkome, G. R.; Moorefield, C. N.; Vögtle, F. *Dendritic Molecules*: *Concepts, Syntheses, Perspectives*; VCH: Weinheim, Germany, 1996. (c) Fischer, M.; Vögtle, F. *Angew. Chem., Int. Ed.* **1999**, *38*, 884.

(2) (a) Hawker, C. J.; Fréchet, J. M. J. *Macromolecules* **1990**, *23*, 4726. (b) Fréchet, J. M. J. *Science* **1994**, *263*, 1710.

(3) Chow, H.-F.; Mong, T. K.-K.; Nongrum, M. F.; Wan, C.-W. *Tetrahedron* **1998**, *54*, 8543.

(4) Majoral, J.-P.; Caminade, A.-M. *Chem. Rev.* **1999**, *99*, 845.

(5) Bosman, A. W.; Janssen, H. M.; Meijer, E. W. *Chem. Rev.* **1999**, *99*, 1665.

(6) Reinhoudt, D. N., Ed. *Supramolecular Materials and Technologies*, *Perspectives in Supramolecular Chemistry*; Wiley: New York, 1999; Vol. 4.

(7) Jiang, D.-L.; Aida, T. *Nature* **1997**, *388*, 454.

(8) Hecht, S.; Fréchet, J. M. J. *Angew. Chem., Int. Ed.* **2001**, *40*, 74.

(9) Zeng, F.; Zimmerman, S. C. *Chem. Rev.* **1997**, *97*, 1681.

(10) Gibson, H. W.; Yamaguchi, N.; Hamilton, L.; Jones, J. W. *J. Am. Chem. Soc.* **2002**, *124*, 4653.

(11) Boas, U.; Söntjens, S. H. M.; Jensen, K. J.; Christensen, J. B.; Meijer, E. W. *ChemBioChem* **2002**, *3*, 433.

(12) Xu, Z.; Moore, J. S. *Acta Polym.* **1994**, *45*, 83.

(13) Gilat, S. L.; Adronov, A.; Fréchet, J. M. J. *Angew. Chem., Int. Ed.* **1999**, *38*, 1422.

(14) Hahn, U.; Gorka, M.; Vögtle, F.; Vicinelli, V.; Ceroni, P.; Maestri, M.; Balzani, V. *Angew. Chem., Int. Ed.* **2002**, *41*, 3595.

(15) (a) Devadoss, C.; Bharathi, P.; Moore, J. S. *J. Am. Chem. Soc.* **1996**, *118*, 9635. (b) Kopelman, R.; Shortreed, M.; Shi, Z.-Y.; Tan, W.; Xu, Z.; Moore, J. S.; Bar-Haim, A.; Klafter, J. *Phys. Rev. Lett.* **1997**, *78*, 1239. (c) Shortreed, M. R.; Swallen, S. F.; Shi, Z.-Y.; Tan, W.; Xu, Z.; Devadoss, C.; Moore, J. S.; Kopelman, R. *J. Phys. Chem. B* **1997**, *101*, 6318.

(16) Kleiman, V. D.; Melinger, J. S.; McMorrow, D. *J. Phys. Chem. B* **2001**, *105*, 5595.

(17) (a) Tretiak, S.; Chernyak, V.; Mukamel, S. *J. Phys. Chem. B* **1998**, *102*, 3310. (b) Kirkwood, J. C.; Scheurer, C.; Chernyak, V.; Mukamel, S. *J. Chem. Phys.* **2001**, *114*, 2419. (c) Tortschanoff, A.; Mukamel, S. *J. Phys. Chem. A* **2002**, *106*, 7521. (d) Tretiak, S.; Mukamel, S. *Chem. Rev.* **2002**, *102*, 3171.

(18) (a) Nakano, M.; Takahata, M.; Fujita, H.; Kiribayashi, S.; Yamaguchi, K. *Chem. Phys. Lett.* **2000**, *323*, 249. (b) Nakano, M.; Takahata, M.; Fujita, H.; Kiribayashi, S.; Yamaguchi, K. *J. Phys. Chem. A* **2001**, *105*, 5473. (c) Nakano, M.; Fujita, H.; Takahata, M.; Yamaguchi, K. *J. Am. Chem. Soc.* **2002**, *124*, 9648. (d) Takahata, M.; Nakano, M.; Fujita, H.; Yamaguchi, K. *Chem. Phys. Lett.* **2002**, *363*, 422.

(19) Yoshizawa, K.; Hoffmann, R. *Chem. Eur. J.* **1995**, *1*, 403.

(20) Shimoi, Y.; Friedman, B. A. *Chem. Phys.* **1999**, *250*, 13.

(21) Hückel, E. *Z. Phys.* **1931**, *70*, 204.

(22) Hohenberg, P.; Kohn, W. *Phys. Rev.* **1964**, *136*, B864.

(23) Kohn, W.; Sham, L. J. *Phys. Rev.* **1965**, *140*, A1133.

(24) Bauernschmitt, R.; Ahlrichs, R. *Chem. Phys. Lett.* **1996**, *256*, 454.

(25) Casida, M. E.; Jamorski, C.; Casida, K. C.; Salahub, D. R. *J. Chem. Phys.* **1998**, *108*, 4439.

(26) Stratmann, R. E.; Scuseria, G. E.; Frisch, M. J. *J. Chem. Phys.* **1998**, *109*, 8218.

(27) Fujimoto, H.; Hoffmann, R. *J. Phys. Chem.* **1974**, *78*, 1167.

(28) Stewart, J. J. P. *J. Comput. Chem.* **1989**, *10*, 209.

(29) Frisch, M. J.; Trucks, G. W.; Schlegel, H. B.; Scuseria, G. E.; Robb, M. A.; Cheeseman, J. R.; Zakrzewski, V. G.; Montgomery, J. A., Jr.; Stratmann, R. E.; Burant, J. C.; Dapprich, S.; Millam, J. M.; Daniels, A. D.; Kudin, K. N.; Strain, M. C.; Farkas, O.; Tomasi, J.; Barone, V.; Cossi, M.; Cammi, R.; Mennucci, B.; Pomelli, C.; Adamo, C.; Clifford, S.; Ochterski, J.; Petersson, G. A.; Ayala, P. Y.; Cui, Q.; Morokuma, K.; Malick, D. K.; Rabuck, A. D.; Raghavachari, K.; Foresman, J. B.; Cioslowski, J.; Ortiz, J. V.; Stefanov, B. B.; Liu, G.; Liashenko, A.; Piskorz, P.; Komaromi, I.; Gomperts, R.; Martin, R. L.; Fox, D. J.; Keith, T.; Al-Laham, M. A.; Peng, C. Y.; Nanayakkara, A.; Gonzalez, C.; Challacombe, M.; Gill, P. M. W.; Johnson, B.; Chen, W.; Wong, M. W.; Andres, J. L.; Head-Gordon, M.; Replogle, E. S.; Pople, J. A. *Gaussian 98*; Gaussian Inc.: Pittsburgh, PA, 1998.

(30) Fukui, K.; Yonezawa, T.; Shingu, H. *J. Chem. Phys.* **1952**, *20*, 722.

(31) (a) Becke, A. D. *Phys. Rev. A* **1988**, *38*, 3098. (b) Becke, A. D. *J. Chem. Phys.* **1993**, *98*, 5648. (c) Lee, C.; Yang, W.; Parr, R. G. *Phys. Rev. B* **1988**, *37*, 785.

(32) (a) Ditchfield, R.; Hehre, W. J.; Pople, J. A. *J. Chem. Phys.* **1971**, *54*, 724. (b) Hehre, W. J.; Ditchfield, R.; Pople, J. A. *J. Chem. Phys.* **1972**, *56*, 2257.

(33) Hariharan, P. C.; Pople, J. A. *Theor. Chim. Acta* **1973**, *28*, 213.